Available online at www.sciencedirect.com
ScienceDirect
Medical Engineering & Physics 29 (2007) 718–727
Medical Engineering & Physics
www.elsevier.com/locate/medengphy

Finite element analysis of the penetrations of shear and normal vibrations into the soft tissues in a fingertip

John Z. Wu*, Daniel E. Welcome, Kristine Krajnak, Ren G. Dong

National Institute for Occupational Safety & Health, Morgantown, WV 26505, USA

Received 17 March 2006; received in revised form 30 June 2006; accepted 4 July 2006

Abstract

It is well accepted that the effects of mechanical vibration on the finger–hand–arm system are strongly frequency-dependent: low frequency vibration can transmit from hand to arm, while high frequency vibration is absorbed in the local tissue of fingers. This assertion has not been validated directly. The purpose of the present study is to analyze the frequency- and deformation-dependent dynamic strains in the soft tissues in a fingertip that is subjected to vibration normal or tangential to the contact surface. The dynamic responses of the fingertip were analyzed using a multi-layered two-dimensional finite element model. The major anatomical substructures, i.e., skin, subcutaneous tissue, bone, and nail, are included in the model. The fingertip was found to have a major resonance around 100–125 Hz and a second resonance around 250 Hz. The resonances of the fingertip are found to be independent of the direction of exposure (in normal or shear direction). The simulations further indicated that the dynamic strains induced by the vibration at low frequencies will penetrate deeper into the tissue (>3 mm) while that at high frequencies will be concentrated in the superficial skin layer (<0.8 mm). The model predictions are consistent with the published experimental observations.

Keywords: Power tool; Soft tissue mechanics; Frequency-domain; Viscoelasticity; Modal analysis

1. Introduction

Extended exposure to hand–arm vibration through the use of tools such as grinders, chipping hammers, and rock drills, could result in hand-arm vibration syndrome (HAVS), the consequences of an array of vascular, sensorineural and musculoskeletal disorders. The most common clinical manifestations of HAVS are the vascular symptoms which present as cold-induced reductions in blood flow and blanching of the skin, together with tingling and numbness of the exposed fingers–hand [1]. Although the mechanisms underlying the development of HAVS are unclear, it is generally believed that vibration induces excessive dynamic loading on soft tissues (e.g., [2–4]). It is well accepted that the effects of mechanical vibration on the finger-hand-arm system is strongly frequency-dependent: low frequency vibration can transmit from hand to arm, while high frequency vibration is absorbed in the local tissue of fingers [5–7]. This assertion has been supported by our previous test results of the vibration distribution in hands and fingers [8,9], which indicated that high frequency vibration energy (>100 Hz) is absorbed in fingers while the low frequency vibration (<40 Hz) is transmitted from palm into arm. The distributions of the dynamic stress/strain in the soft tissues during vibration exposure have, however, not been evaluated directly because of technical difficulties in measuring these effects on soft tissues.

In occupational settings, the vibrations produced by handheld tools are always three-dimensional. However, in both experimental studies [10] and theoretical [11] analyses, the vibrations were usually considered as uniaxial in a direction normal to the contact surface. The response of hand–fingers to the shear vibration has rarely been characterized [12]. Previous studies suggest that the response of a fingertip to a dynamic load applied in the normal direction is quite different from that applied in a shear direction [13]; correspondingly, the perception of fingers to the vibration in normal direc-

* Corresponding author. Tel.: +1 304 285 5832; fax: +1 304 285 6265.
E-mail address: jwu@cdc.gov (J.Z. Wu).

1350-4533/$ – see front matter © 2006 IPEM. Published by Elsevier Ltd. All rights reserved.
doi:10.1016/j.medengphy.2006.07.005

tion by a subject is also different from that in shear direction [14].

Soft tissues show different physiological responses to shear and normal stress. For example, lower levels of shear stress eventually result in the remodeling of peripheral nerves, and an increase in their resiliency [15], while higher levels of shear can result in nerve tears [16,17]. In contrast, normal or compressive stresses can result in damage to both the myelin sheath and axons of peripheral nerves [18–21]. Skin is more resilient to shear stress because an underlying collagen layer allows the skin to slide independently of the underlying tissue [22]. However, exposure to cyclic shear stress does result in skin damage in animals that have been tested [23]. Finally, in blood vessels, exposure to both shear and normal stresses may produce similar effects on vascular physiology. Mechanically induced changes in vascular shape in response to stress alter shear forces produced by blood flow through the vessels. These alterations in fluid shear stress on endothelial cells mediate remodeling of blood vessels [24–27]. Thus, the overall physiological responses and the soft tissue damage induced by mechanical loading are different for shear and normal stress.

A fingertip is composed of skin layers (epidermis and dermis), subcutaneous tissue, bone, and nail. The hard tissues (i.e., bone and nail) are typically elastic, while the soft tissues (i.e., skin and subcutaneous tissues) are nonlinear and viscous [28,29]. When the finger is in contact with an object, the mechanical vibrations are transferred through the skin and subcutaneous tissues to hand, arm, and body. Because of the nonlinear and time-dependent mechanical properties of the soft tissues, the transmission of the vibration in the fingers is dependent on the frequency and finger deformations. The mechanical responses of fingers to static [30] and dynamic loading [31] have been studied by several researchers. However, the responses of the soft tissues in the finger to vibration have seldom been analyzed.

In order for engineers to improve the tool design to reduce hand–arm vibration injuries, we have to understand how the vibrations transfer from the handle of the power-tool into the soft tissues of the fingers. The present study is intended to analyze the frequency- and deformation-dependent dynamic strains in the soft tissues in fingertip that is subjected to vibrations in a direction normal or tangential to the contact surface. Specifically, the distributions of the vibration-induced dynamic strains in the soft tissue of the fingertip are to be simulated. The fingertip will be compressed statically to different deformation states before being subjected to the normal or shear vibrations. The main purpose of the study is to investigate: (a) the difference between the distributions of the dynamic strains induced by the shear vibration and those induced by the normal vibration, and (b) the effects of the static compression on the dynamic strains in the soft tissues. The numerical simulations are performed using a nonlinear two-dimensional finite element (FE) model, which includes major anatomical substructures: skin layers, subcutaneous tissue, bone, and nail.

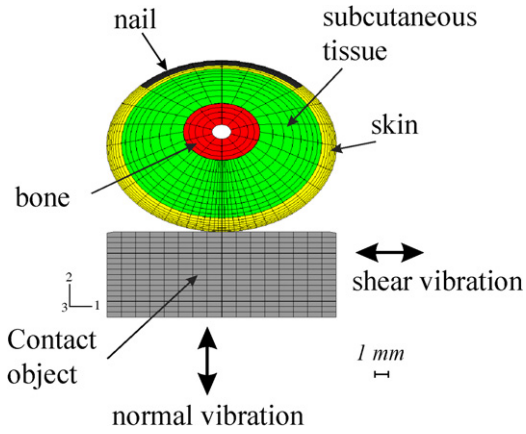

Fig. 1. Two-dimensional (2D) finite element model of a fingertip in contact with a flat surface. A cross section of the fingertip is modeled using the 2D finite element model. The center of the fingernail was supported while the fingerpad was activated by a vibrating plate. The fingertip was composed of skin, subcutaneous tissue, bone, and nail; the skin and subcutaneous tissues were assumed to be nonlinearly elastic and viscoelastic. The flat contact surface was considered to be of PVC polymer, which was assumed to be linearly elastic. The contact plate was subjected to normal and shear vibrations.

2. Methods

2.1. FE model

The dynamic responses of the fingertip were analyzed using a multi-layered two-dimensional (2D) finite element model, as shown in Fig. 1. The fingertip was assumed to be composed of a skin layer (representing epidermis and dermis), subcutaneous tissue, bone, and nail. The fingertip was assumed to have a width of 16 mm and a height of 12 mm, dimensions typical for an index finger [32]. The skin was assumed to have a thickness of 0.8 mm [33]. Both skin, including epidermis and dermis, and subcutaneous tissues were assumed to be nonlinearly elastic and viscoelastic. The nail, bone, and contacting objects were considered as linearly elastic. The center of the fingernail was supported while the fingerpad was in contact with a flat surface, which was assumed to be of polyvinyl chloride (PVC) polymer. PVC is considered as a common material for typical tool handles. The friction coefficient between the contact surface and the finger skin is assumed to be 0.5. The simulations were performed using a commercial finite element software package, Abaqus (Version 6.4). The FE model and the material models of the soft tissues are described in detail in our previous work [34].

2.2. Simulation procedure

The simulation was performed in two stages. First, the contact plate was displaced towards the finger to achieve a predetermined value of tissue deformation (i.e., 0.5, 1.0, 1.5, and 2.0 mm). The material and geometric nonlinearities are considered in the static compression. Secondly, the fingertip is subjected to a continuous harmonic excitation (with a displacement magnitude of 0.5 mm) from the contact

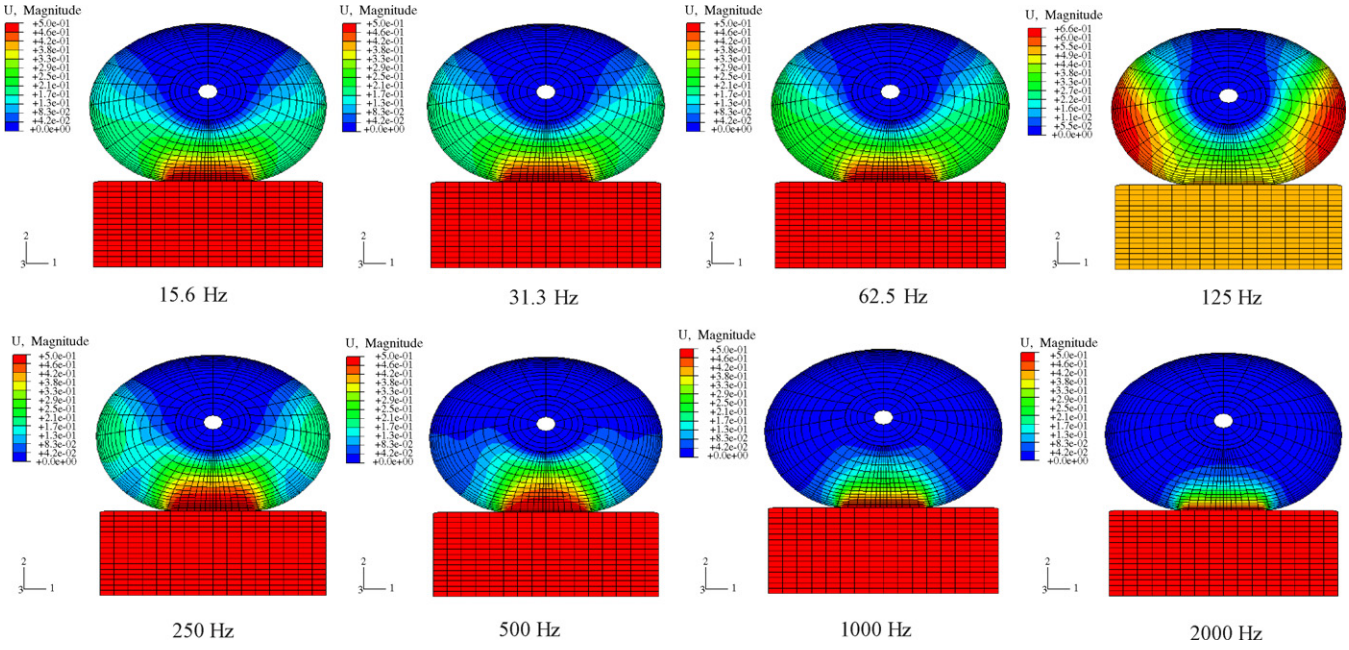

Fig. 2. The distributions of vibration magnitude (U, mm) across the tissues of a fingertip subjected to normal vibration. The fingertip is pre-compressed by (d_0 =) 1 mm before being subjected to harmonic vibrations, and results shown are for eight different vibration frequencies (f = 16, 32, 63, 125, 250, 500, 1000, and 2000 Hz). The figures show that the contacting plate was specified to the same displacement at all frequencies, while the distributions of the vibration magnitude within the tissues vary as a function of the frequency. At 125 Hz, the vibration magnitude in the tissues substantially exceeds that specified on the contacting plate.

interface. The vibrations were applied in directions normal and tangential to the contact surface separately (Fig. 1). The analysis is performed using a linear perturbation procedure. The fingertip is assumed to undergo small harmonic vibrations around the deformed, stressed state, and the perturbed solutions are calculated using the tangential stiffness at the deformed state [35,36]. Since the harmonic vibration is considered to be infinitesimal, the contact area is assumed

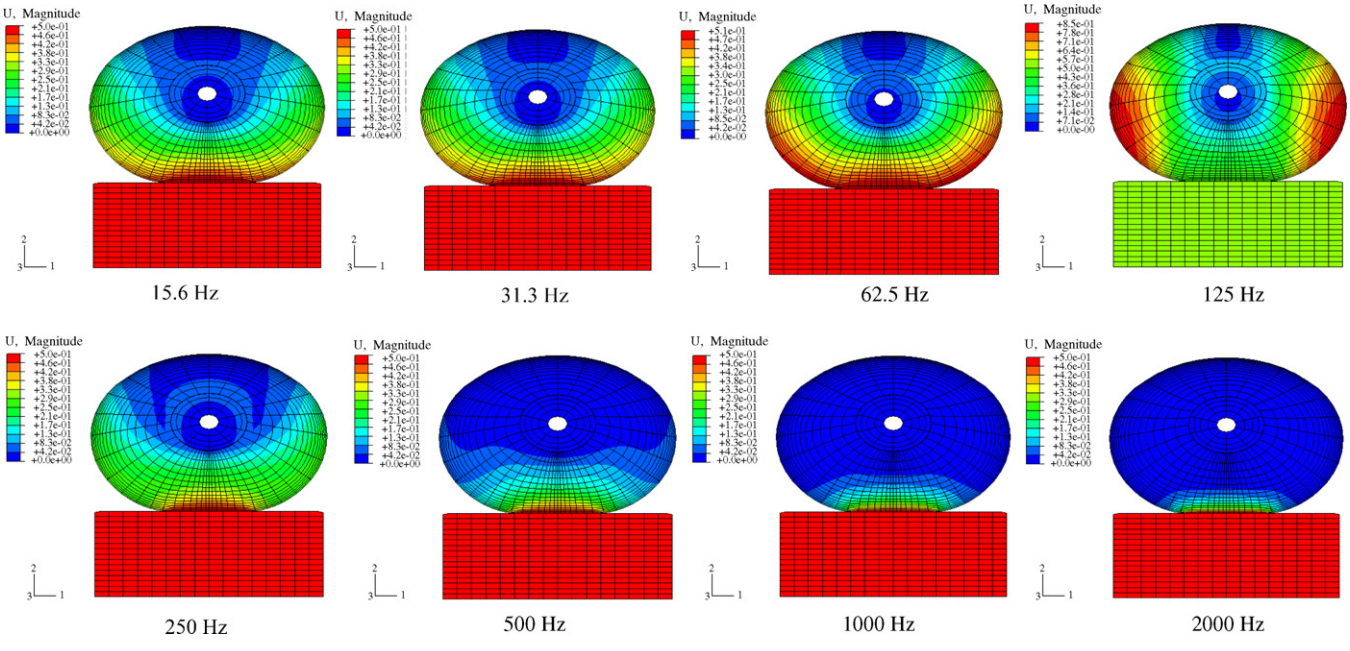

Fig. 3. The distributions of vibration magnitude (U, mm) across the tissues of a fingertip subjected to shear vibration. The fingertip is pre-compressed by (d_0 =) 1 mm before being subjected to harmonic vibrations, and results shown are for eight different vibration frequencies (f = 16, 32, 63, 125, 250, 500, 1000, and 2000 Hz). The figures show that the contacting plate was specified to the same displacement at all frequencies, while the distributions of the vibration magnitude within the tissues vary as a function of the frequency. At 125 Hz, the vibration magnitude in the tissues substantially exceeds that specified on the contacting plate.

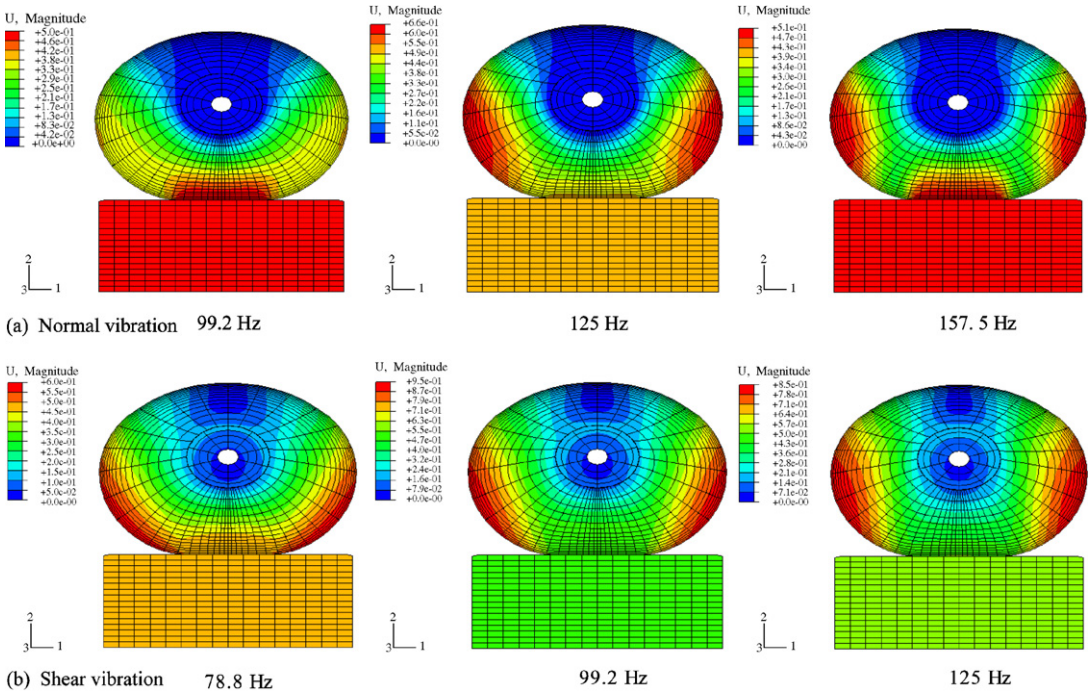

Fig. 4. The distributions of vibration magnitude (U, mm) across the tissues of a fingertip around the major resonance. (a) Normal vibration. (b) Shear vibration. The fingertip is pre-compressed by (d_0 =) 1 mm before being subjected to harmonic vibrations. The vibration magnitudes in the tissues reach peaks around 125 and 99.2 Hz for normal and shear vibrations, respectively, indicating that the fingertip has resonances around these frequencies.

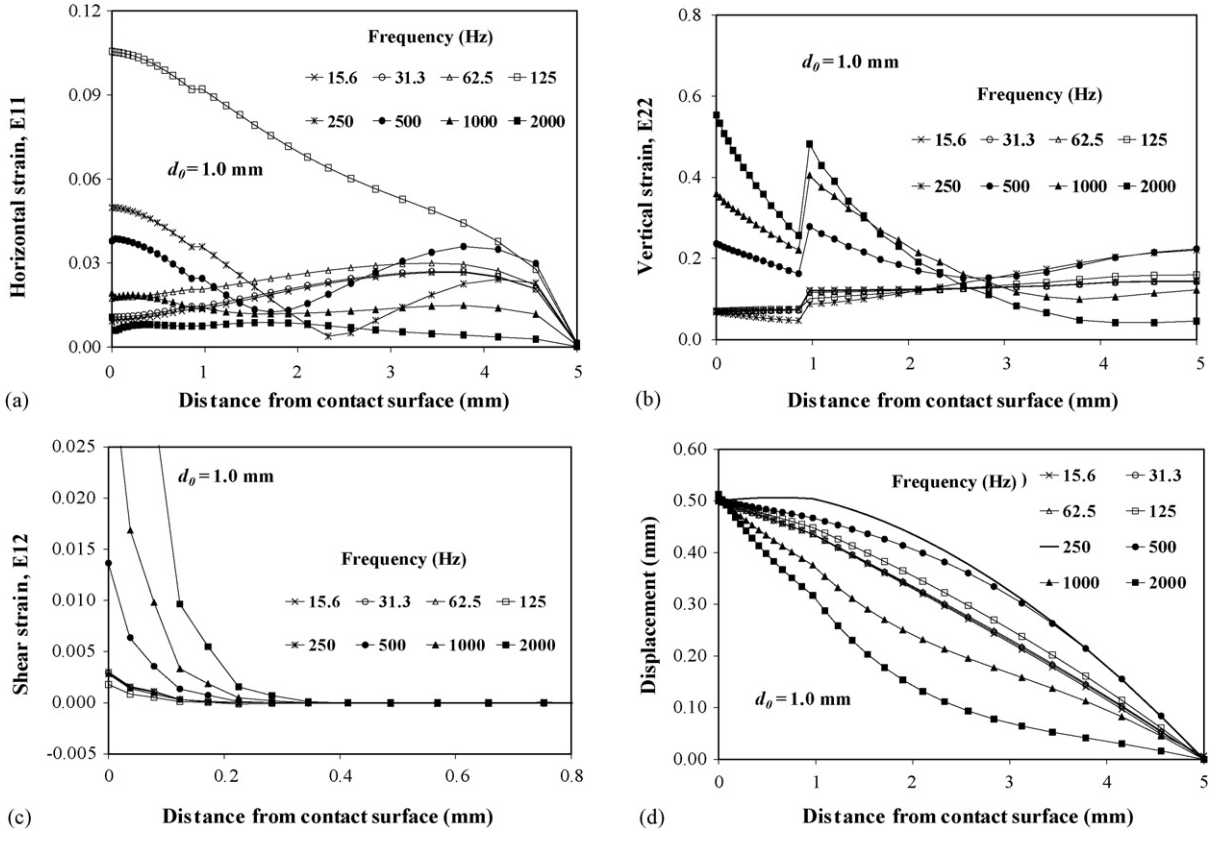

Fig. 5. The distributions of dynamic stains (E_{11}, E_{22}, E_{12}) and vibration magnitude across the tissues of a fingertip subjected to normal vibration. The fingertip is pre-compressed by (d_0 =) 1 mm before being subjected to harmonic vibrations, and results shown are for eight different vibration frequencies (f = 16, 32, 63, 125, 250, 500, 1000, and 2000 Hz).

to be unchanged during the vibrations. The stiffness of the soft tissues in the fingertip is location- and pre-deformation-dependent, due to the nonlinearly elastic properties of the soft tissue and the geometric nonlinearities. The dynamic analysis is performed in a frequency range from 16 to 2000 Hz in octave band intervals. The frequency-dependent distributions of the vibration magnitude and dynamic strain magnitudes across the soft tissues are investigated.

In this two-dimensional model, there are only three strain components, i.e., ε_{11}, ε_{22}, and ε_{12}. In order to study the distributions of the dynamic strain concentrations, an equivalent strain, ε_{eqv}, is defined [37]:

$$\varepsilon_{\text{eqv}} = \sqrt{\frac{2}{3}\varepsilon_{ij}\varepsilon_{ij}}, \quad i, j = 1, 2 \tag{1}$$

For a linear harmonic vibration, the vibration (displacement) magnitude, u_0, is related to the magnitude of the dynamic speed and acceleration, v_0 and a_0, by $v = \omega u_0$ and $a = \omega^2 u_0$, respectively. For tests with a constant velocity, v_0, the applied vibration magnitude decreases with vibration frequency, $u(\omega) = v_0/\omega$; while for tests with a constant acceleration, a_0, the applied vibration magnitude decreases with square of vibration frequency, $u(\omega) = a_0/\omega^2$. During the harmonic vibration of the fingertip, the variations of the internal displacements and strains are strictly proportional to the applied displacement at the contact interface. Therefore, the internal displacements and strains for constant acceleration tests can be calculated from the results obtained for constant displacement tests by linear scaling. In the present studies, the numerical tests are performed using a constant vibration magnitude (0.5 mm). The equivalent strains for the constant-displacement tests (ε_{eqv}) are then converted to those for the constant velocity and constant acceleration tests by $\varepsilon_{\text{eqv}}/\omega$ and $\varepsilon_{\text{eqv}}/\omega^2$, respectively. The same material models and parameters as those used in our previous [34] have been applied in the current analysis.

3. Results

The predicted distributions of the vibration magnitude across the fingertip, subjected to the vibrations normal and tangential to the contact surface, are depicted in Figs. 2 and 3, respectively. In these tests, the fingertip was pre-compressed by 1 mm before being applied to vibrations. The vibration distributions across the finger section are illustrated in color scales in these figures. It is seen that the vibration magnitudes of the contacting plate for all cases are the same, while the distributions of the vibration magnitude

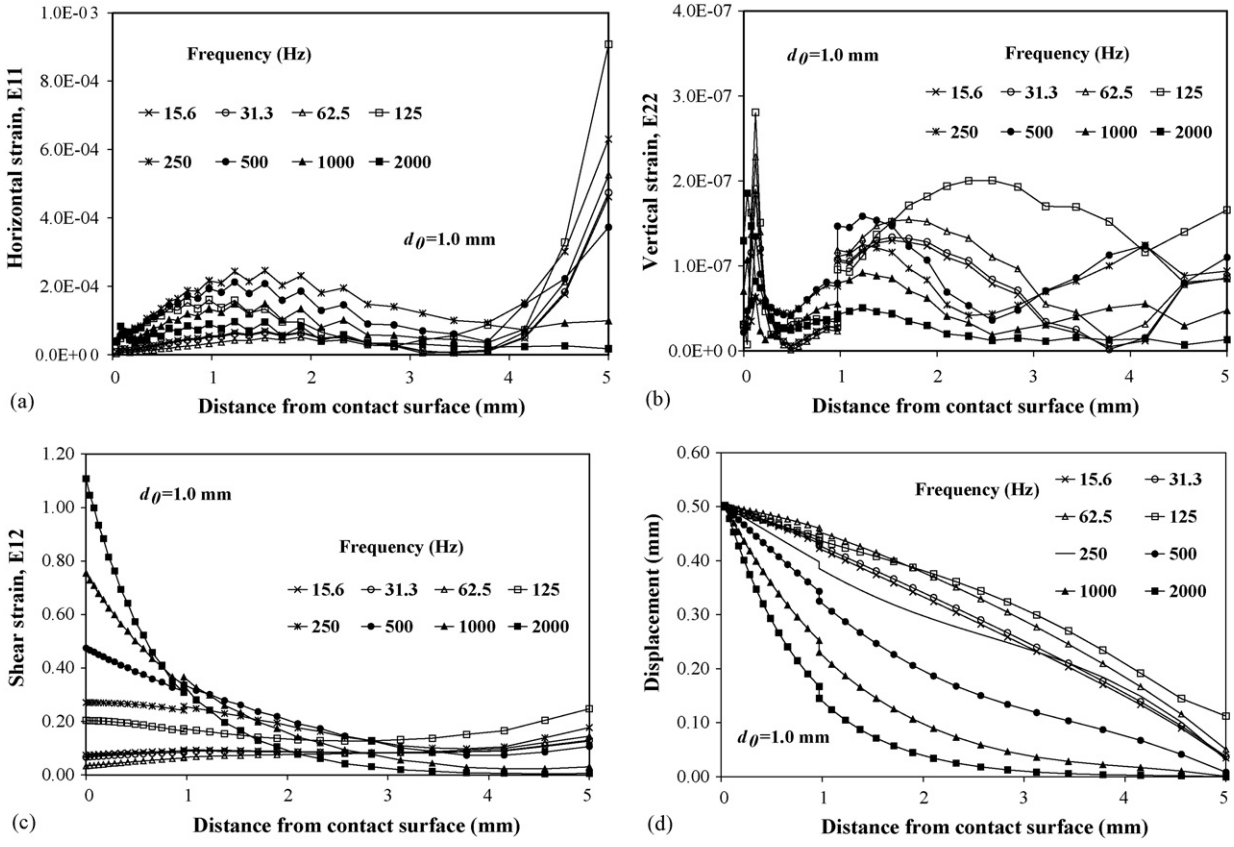

Fig. 6. The distributions of dynamic stains (E_{11}, E_{22}, E_{12}) and vibration magnitude across the tissues of a fingertip subjected to shear vibration. The fingertip is pre-compressed by (d_0 =) 1 mm before being subjected to harmonic vibrations, and results shown are for eight different vibration frequencies (f = 16, 32, 63, 125, 250, 500, 1000, and 2000 Hz).

across the finger section vary with vibration frequency. At a frequency of 125 Hz, the vibration magnitudes in the soft tissues substantially exceed that specified on the vibrating plate, indicating that the finger reaches the resonance around that frequency. It is seen from the results of both normal and shear vibrations, that the penetration of the vibration into the soft tissues increases with increasing frequency before the resonance of 125 Hz; while at frequencies higher than the resonance, the penetration of the vibration into the tissues decreases with the increasing frequencies.

In order to investigate the resonant characteristics of the fingertip under normal and shear vibrations, the simulations (Figs. 2 and 3) were repeated at a refined interval around the resonance (125 Hz), as shown in Fig. 4. The vibration magnitudes in the tissues peaks around 125 Hz (Fig. 4a) and 99.2 Hz (Fig. 4b) for normal and shear vibrations, respectively, indicating that the fingertip has resonances around these frequencies.

The results of the modal pattern characteristics are quantitatively analyzed to show the distributions of the strains and vibration magnitude across the soft tissues at eight different frequencies, as in Figs. 5 and 6. In these figures, the distance from the contact surface (the horizontal axis) is calculated from the un-deformed state and along the centerline of the fingertip. The value "0 mm" is at the contact surface, while "5 mm" is at the interface between bone and subcutaneous tissue.

For the tests with the normal vibration, the distributions of the vibration magnitude are shown in Fig. 5(d), while the corresponding distributions of the strain components, ε_{11}, ε_{22}, and ε_{12}, are shown in parts (a), (b), and (c), respectively, of Fig. 5. It is interesting to see that the characteristics of strain distributions are quite different for different strain components. The value of the horizontal strain (ε_{11}) at 125 Hz is much higher than those for other frequencies (Fig. 5(a)). The vertical strain (ε_{22}) shows a sudden variation around the transition of skin/subcutaneous tissue. In the region near the skin surface (<0.8 mm) and for frequency above 500 Hz, the value of ε_{22} increases substantially with increasing frequency (Fig. 5(b)). In the superficial skin layer (<0.2 mm) and for frequencies above 250 Hz, the shear strain (ε_{12}) increases dramatically with increasing frequency; while the shear strain is negligible deep in the tissue (>0.3 mm) for all frequencies (Fig. 5(c)). The overall value of the vibration magnitude in the tissue reaches the maximum at 250 Hz (Fig. 5(d)). Deep in the tissue (>2.5 mm) and for frequencies above

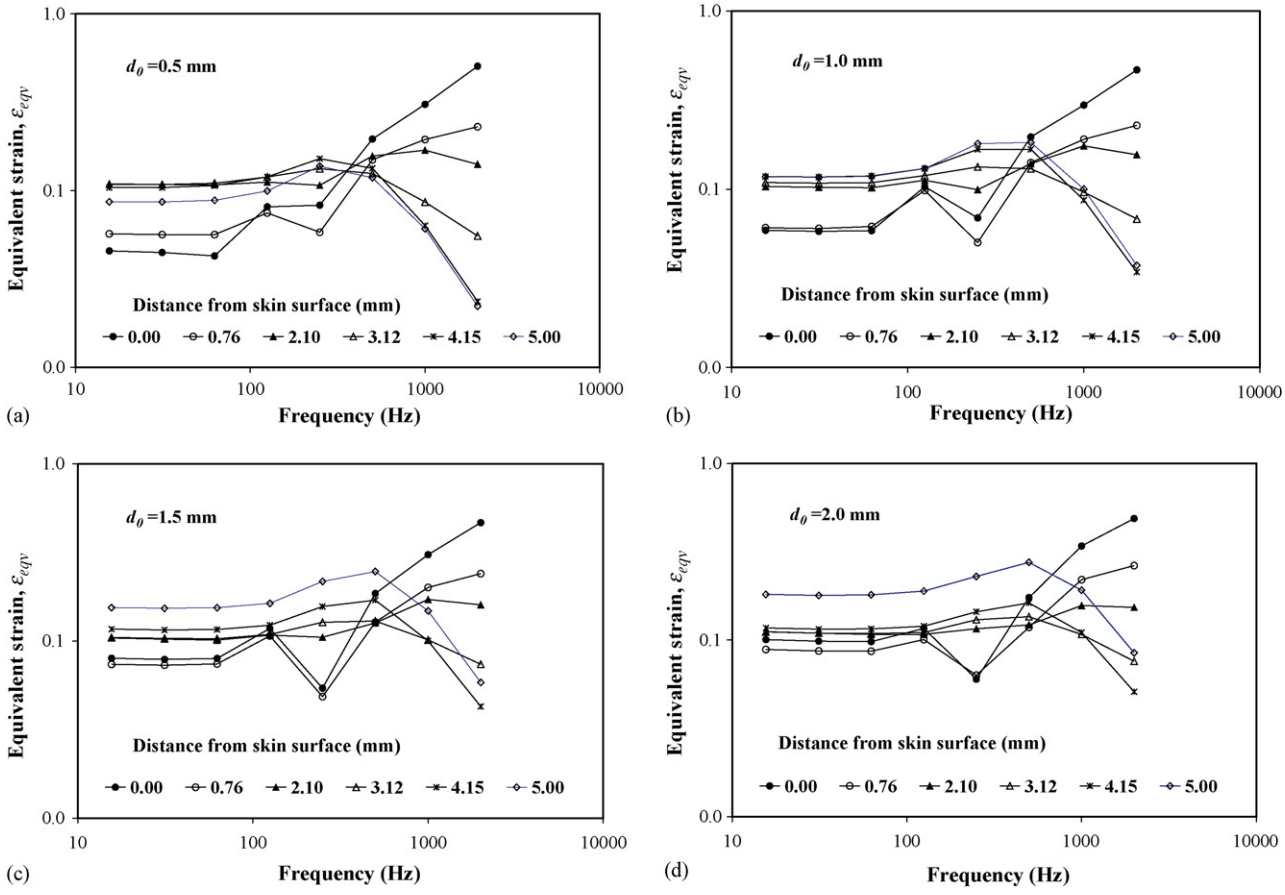

Fig. 7. The effective strain magnitude (ε_{eqv}) at six different tissue depths (0.0, 0.76, 2.1, 3.12, 4.15, and 5.0 mm) as a function of vibration frequency for tests of normal vibration. These results are for the vibration tests performed using constant displacement. (a), (b), (c), and (d) are for pre-compressions (d_0) of 0.5, 1.0, 1.5, and 2.0 mm, respectively.

250 Hz, the vibration magnitude decreases with increasing frequency.

For the tests with the shear vibration, the distributions of the strain components, ε_{11}, ε_{22}, and ε_{12}, and vibration magnitude across the tissue are shown in parts (a), (b), (c), and (d), respectively, of Fig. 6. It is seen that the magnitude of the strains in both horizontal and vertical directions (ε_{11} and ε_{22}, as shown in parts (a) and (b), respectively, of Fig. 6) are small compared to the shear strain (ε_{12}, as shown in Fig. 6(c)). Around the transition of skin/subcutaneous tissue, the curves for the vertical strain and magnitude, as depicted in parts (b) and (d), respectively, of Fig. 6, show sudden variations. In the superficial skin layer (<1 mm), the shear strain first decreases with increasing frequency (<62.5 Hz), suddenly increases at the resonance (around 125 Hz), and then increases dramatically with increasing frequency (>250 Hz). At the contact surface the vibration magnitude is prescribed at 0.5 mm, while its distribution across the tissue varies with frequency: the vibration magnitude first increases with increasing frequency (<62.5 Hz), reaches the maximum at 125 Hz, and then decreases with increasing frequency (>250 Hz).

In order to evaluate the combined effects of all strain components across the tissues, the frequency-dependent equivalent strain (ε_{eq}) at six different tissue depths for pre-compression (d_0) of 0.5, 1.0, 1.5, and 2.0 are plotted in parts (a), (b), (c), and (d), respectively, of Figs. 7. These numerical tests were performed using normal vibration. At high frequency, the equivalent strain in the superficial zone is much higher than that in the deep zone; while at low frequency, the equivalent strain is quite uniformly distributed across the tissue. The effect of the pre-compression on the dynamic strain distribution in the tissue seems both location and frequency-dependent. At low frequency (<62.5 Hz), the dynamic strains across the tissue tend to increase with increasing pre-compression. At high frequency (>500 Hz), the dynamic strain in the deep layer (>3.12 mm) increases with increasing pre-compression, while those in the superficial layer (<0.8 mm) is less influenced. In general, the pre-compression tends to make the distribution of the dynamic strain more uniform across the tissue.

All results shown in Figs. 5–7 were obtained in numerical tests with a constant vibration magnitude of 0.5 mm. In many practical applications, vibration tests have been performed using constant velocity and constant acceleration. Therefore, the distributions of the equivalent strain (as in Fig. 7), ε_{eqv}, have been normalized to ε_{eqv}/ω and $\varepsilon_{eqv}/\omega^2$ and shown in Figs. 8 and 9, respectively. It is seen that the magnitude of the normalized equivalent strains, ε_{eqv}/ω and $\varepsilon_{eqv}/\omega^2$, at

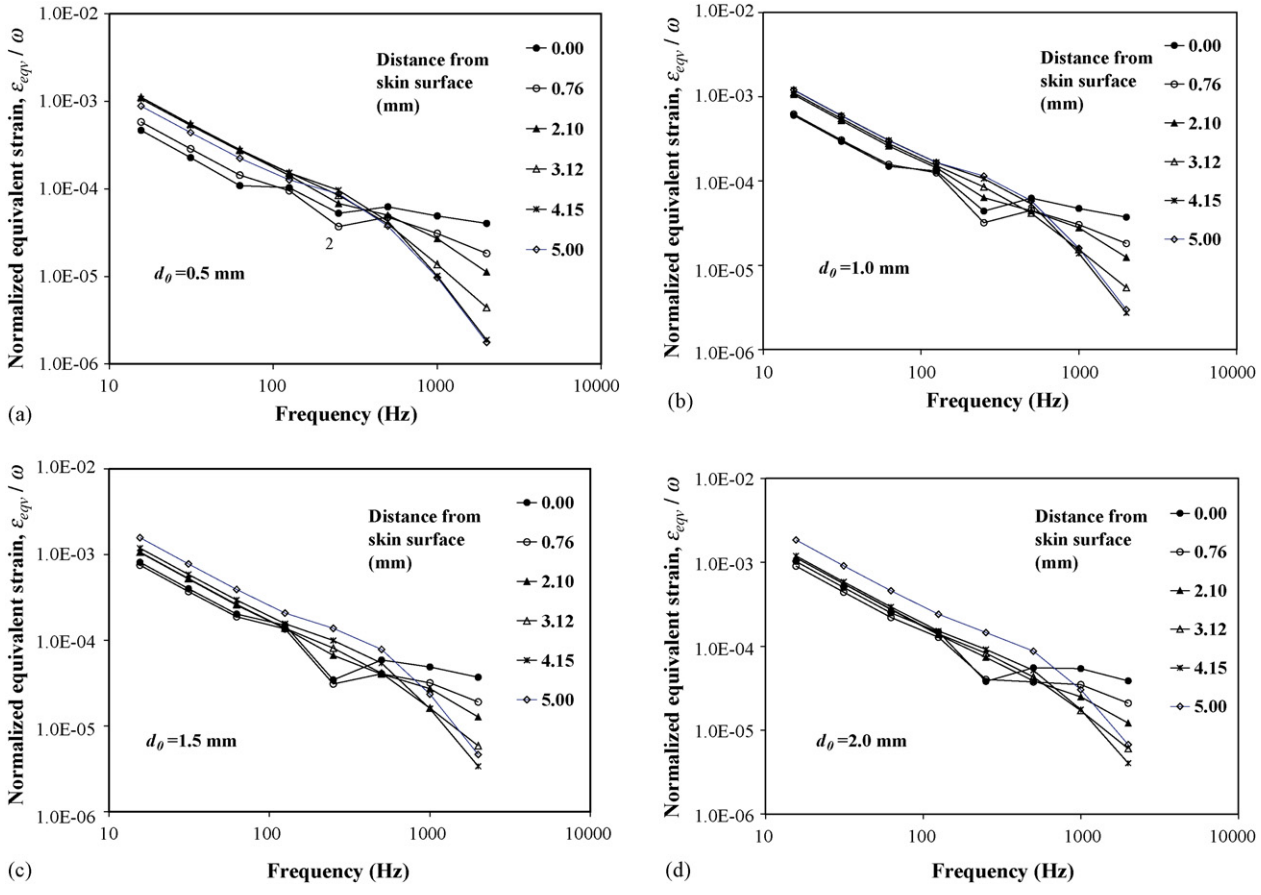

Fig. 8. The normalized effective strain magnitude (ε_{eqv}/ω, s) at six different tissue depths (0.0, 0.76, 2.1, 3.12, 4.15, and 5.0 mm) as a function of vibration frequency for tests of normal vibration. These results are corresponding to the vibration tests performed using constant velocity. (a), (b), (c), and (d) are for pre-compressions (d_0) of 0.5, 1.0, 1.5, and 2.0 mm, respectively.

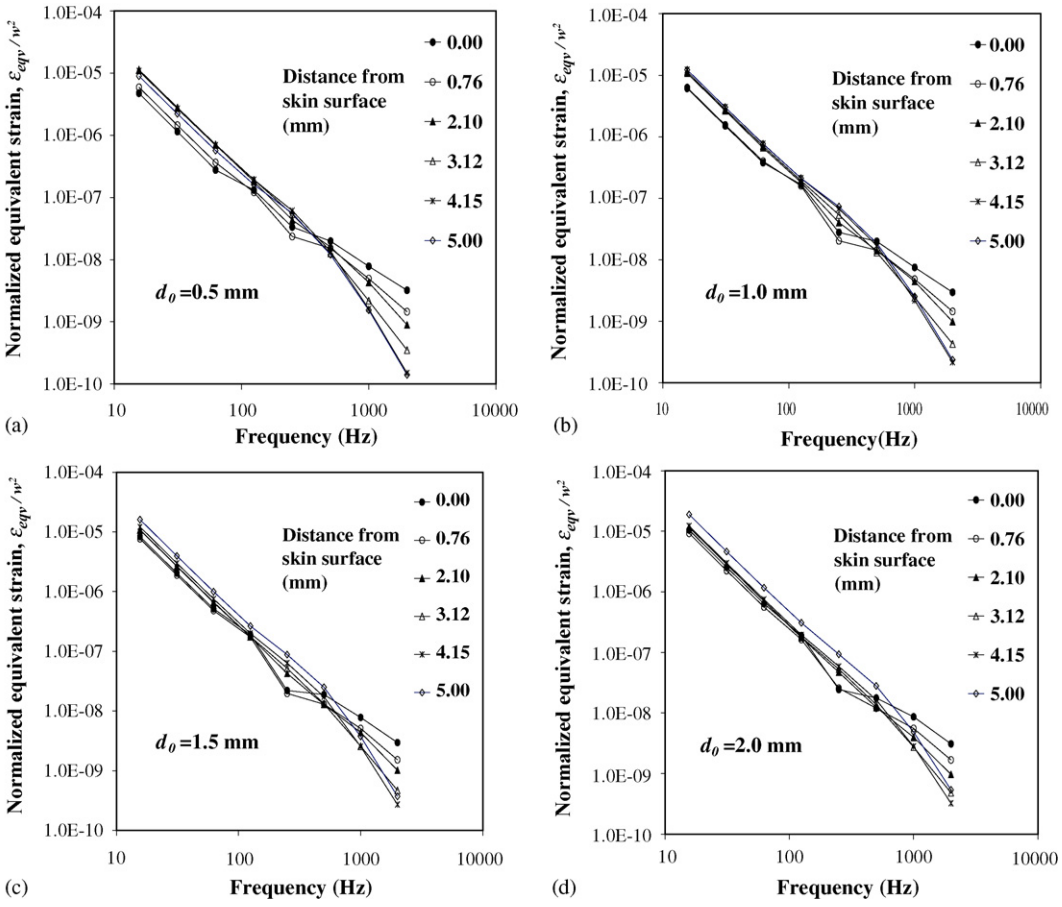

Fig. 9. The normalized effective strain magnitude ($\varepsilon_{eqv}/\omega^2$, s^2) at six different tissue depths (0.0, 0.76, 2.1, 3.12, 4.15, and 5.0 mm) as a function of vibration frequency for tests of normal vibration. These results are corresponding to the vibration tests performed using constant acceleration. (a), (b), (c), and (d) are for pre-compressions (d_0) of 0.5, 1.0, 1.5, and 2.0 mm, respectively.

different depths decrease consistently with increasing frequency. The pre-compression on the fingerpad tends to make the distribution of the normalized equivalent strains more frequency-independent deep in the tissue (>3.0 mm). The strains at the superficial layer appear to be little influenced by the pre-compression. Around a frequency of 250 Hz, the distributions of the effective dynamic strains across the tissue (Figs. 7–9) show a dip that is independent of the levels of pre-compression. These observations indicate that there is a second resonance of the fingertip around 250 Hz.

4. Discussion and conclusion

Although the dynamic stress and strain in the soft tissues are believed to result in degeneration and dysfunction in the vascular and neural systems in the fingers, a direct link between occupational exposures to vibration, and the development of hand disorders has not been established. The effects of mechanical vibration on the neural and vascular systems depends on the degree of finger deformation in response to vibration frequency [38–40]. In the present study, we theoretically analyzed the frequency-dependent distributions of dynamic strain in the soft tissues in a fingertip that is subjected to normal and shear vibration. The current simulation indicated that vibration at low frequencies will penetrate into tissue, while at high frequencies it will be absorbed in the skin surface. These model predictions are consistent with experimental observations [8,9]. The knowledge of the vibration penetration into the soft tissue of the finger obtained in the present study will help to understand the mechanisms of HAVS and optimize designing of hand-held tools to reduce occupation-related disorders of the hand.

It is interesting to observe that the shear vibration induces significant shear strains and negligible normal strains in soft tissue, while the normal vibration induces both normal and shear strains in the tissues. The combined normal and shear strain induced by normal vibration may explain why vibration exposure in the plane is so damaging to both neural and vascular tissues [15]. Furthermore, the shear strain caused by the normal vibration is significant only in a superficial skin layer (<0.3 mm) and negligible deep in the tissue (Fig. 5(c)). The shear strains at the superficial layer caused by both normal and shear vibrations are observed to increase dramatically for vibration frequencies above 250 Hz. Shear stresses

may cause significant damage on the skin tissues. However, because the shear strains are concentrated in the superficial skin layer, they may be effectively reduced by using a suitable protection glove.

Our simulation results indicated that the major resonance of the finger is around 100–125 Hz that is independent of the direction of activations (in normal or shear direction). The distributions of the strains and vibration magnitude across the tissue show that, around the resonance of 125 Hz, the magnitude of the horizontal strain, E_{11}, is substantially higher for the normal vibration (Fig. 5a), while the value of the vertical strain, E_{22}, is substantially higher for the shear vibration (Fig. 6b). The predicted major resonance of the finger is consistent with the experimental results obtained in vibration transmissibility tests, which showed a peak in a range of 80–150 Hz [10]. However, the vibration tests can only measure the global mechanical response of the finger and cannot evaluate the responses of the soft tissues. The present study indicated that the resonance at 100–125 Hz is associated with the dramatic increase in the tissue strains.

From the distribution of the dynamic strain across the tissue (Figs. 5–9) one can identify a second resonance around 250 Hz. The distributions of the dynamic strains in tissue for both normal (Fig. 5) and shear vibrations (Fig. 6) indicate that around the second resonance (250 Hz) the magnitude of the horizontal strain in the tissues reaches a peak. This second resonance has been confirmed consistently by the distributions of the effective dynamic strains for the numerical tests with constant vibration magnitude (Fig. 7), constant velocity (Fig. 8), and constant acceleration (Fig. 9). These results further indicate that this second resonance of the fingertip is independent of the pre-compression. This model prediction is consistent with our previous study of the finger mechanical impedance [41], which showed a peak of the energy absorption rate of the fingers around 250 Hz, indicating that dynamic strain values in the soft tissues reach peak around the second resonance. This model prediction suggests that the vibrations around a frequency of 250 Hz may likely cause damage to the neural and vascular systems.

From the present simulations, it is seen that the vibration magnitude across the tissue decreases with increasing frequency for the constant speed or constant acceleration tests. The risk of vibration induced injury or damage on the neural system in finger can, however, not be evaluated solely based on the vibration magnitude. The vibrations applied at the fingertip are detected by the Meissner's and Pacinian corpuscles, which are assumed to be located in superficial (0.2–0.9 mm depth) and deep zone (2.5–4.2 mm depth) [42], respectively. The sensitivity thresholds of these receptors are frequency-dependent. The Meissner's corpuscles are maximally activated in response to low frequency vibrations (less that 60 Hz) or flutter that results in a 50–1000 μm indentation within the skin [43]. In contrast, the Pacinian corpuscles are activated in response to higher frequency vibrations (40–300 Hz) that result in a 1–1000 μm indentation of the skin [43]. In order to evaluate the effects of the vibration on the neural systems in fingertip, both vibration magnitude across the tissue and the frequency-dependent sensitivity of the mechanoreceptors should be taken into account.

Our simulation results indicate that, at very high frequencies (>1000 Hz), the vibration induced dynamic strain is concentrated at a tissue depth less than 1 mm, and vibration energy dissipates at the skin surface layer. Although the vibration at very high frequencies may have few acute effects on the sensory perception, because these mechanical stimuli are well beyond the frequency range of the mechanoreceptors, they may potentially result in the structural damage of the local tissues [44,45].

Our simulation results indicated that the effects of the pre-compression on the dynamic strain distributions across the soft tissue is location and frequency-dependent. The general resonant characteristics are less influenced by the pre-compression. In general, the pre-compression tends to make vibration penetrate deeper into the tissues over the entire frequency range. Based on the present simulations, one would expect that the risk of the vibration damage on the neural and vascular system in fingers would increase with increasing grip force.

The shear vibration is transmitted to the soft tissues through the friction between the skin and vibration plate. We have numerically tested the effects of the friction on the vibration transmission between the finger and contact plate (results not shown). For a friction coefficient of 0.5, there is no relative sliding between the skin and the contact plate in our simulations. For friction coefficient less than 0.1, the finger skin begins to slide relative to the contact surface during vibration. The effect of the friction on the normal vibration transmission is found to be negligible.

In conclusion, in the present study we analyzed, for the first time, the frequency-dependent distributions of dynamic strains in a fingertip subjected to the normal and shear vibrations. The model prediction on the resonant characteristics of the finger is consistent with the published experimental observations. The proposed model can be used to predict the responses of the soft tissues in different depths to vibration exposures, providing valuable information and data that are essential for understanding the mechanism of the vibration-induced hand–finger disorders.

Acknowledgments

The findings and conclusions in this report are those of the authors and do not necessarily represent the views of the National Institute for Occupational Safety and Health (NIOSH).

References

[1] James P, Galloway R. Arteriography of the hand in men exposed to vibration. In: Talor W, Pelmear P, editors. Vibration white finger in industry, vol. 4 . London: Academic Press; 1975. 31–41.

[2] Lindsell C, Griffin M. Thermal thresholds, vibrotactile thresholds and finger systolic blood pressures in dockyard workers exposed to hand-transmitted vibration. Int Arch Occup Environ Health 1999;72(6):377–86.
[3] Bovenzi M, Franzinelli A, Mancini R, Cannava MG, Maiorano M, Ceccarelli F. Dose–response relation for vascular disorders induced by vibration in the fingers of forestry workers. Occup Environ Med 1995;52(11):722–30.
[4] Sakakibara H, Zhu S, Toyoshima H. Effect of vibration magnitude and repetitive exposure on fingertig blood flow in healthy subjects. Int Arch Occup Environ Health 2000;73:281–4.
[5] Pyykko I, Farkkila M, Toivanen J, Korhonen O, Hyvarinen J. Transmission of vibration in the hand–arm system with special reference to changes in compression force and acceleration. Scand J Work Environ Health 1976;2:87–95.
[6] Reynolds D, Angevine EN. Hand–arm vibration, part ii: Vibration transmission characteristics of the hand and arm. J Sound Vib 1977;51:255–65.
[7] Sorensson A, Lundstrom R. Transmission of vibration to the hand. J Low Freq Noise Vib 1992;11:14–22.
[8] Dong RG, Wu JZ, Welcome DE, McDowell TW. Estimation of vibration power absorption density in human fingers. J Biomech Eng 2005;127(5):849–56.
[9] Dong RG, Wu JZ, McDowell TW, Welcome DE, Schopper AW. Distribution of mechanical impedance at the fingers and the palm of the human hand. J Biomech 2005;38(5):1165–75.
[10] Dong RG, Rakheja S, Schopper AW, Han B, Smutz WP. Hand-transmitted vibration and biodynamic response of the human hand–arm: a critical review. Crit Rev Biomed Eng 2001;29(4):393–439.
[11] Rakheja S, Wu JZ, Dong RG, Schopper AW. A comparison of biodynamic model of the human hand–arm system for applications to hand-held power tools. J Sound Vib 2002;249(1):55–82.
[12] Reynolds D, Soedel W. Dynamic response of the hand-arm system to a sinusoidal input. J Sound Vib 1972;21:339–53.
[13] Nakazawa N, Ikeura R, Inooka H. Characteristics of human fingertips in the shearing direction. Biol Cybern 2000;82(3):207–14.
[14] Griffin MJ. Measurement, evaluation, and assessment of occupational exposures to hand-transmitted vibration. Occup Environ Med 1997;54(2):73–89.
[15] Topp K, Boyd B. Structure and biomechanics of peripheral nerves: nerve responses to physical stresses and implications for physical therapist practice. Phys Ther 2006;86:92–109.
[16] Kwan M, Wall E, Massie J, Garfin S. Strain, stress and stretch of peripheral nerve: rabbit experiments in vitro and in vivo. Acta Orthop Scand 1992;63:267–72.
[17] Wall EJ, Massie JB, Kwan MK, Rydevik BL, Myers RR, Garfin SR. Experimental stretch neuropathy. changes in nerve conduction under tension. J Bone Joint Surg Br 1992;74:126–9.
[18] Lundborg G, Dahlin LB. The pathophysiology of nerve compression. Hand Clin 1992;8:215–27.
[19] Lundborg G, Dahlin LB, Danielsen N, Hansson HA, Necking LE, Pyykko I. Intraneural edema following exposure to vibration. Scand J Work Environ Health 1987;13(4):326–9.
[20] Lundborg G, Dahlin LB, Hansson HA, Kanje M, Necking LE. Vibration exposure and peripheral nerve fiber damage. J Hand Surg [Am] 1990;15(2):346–51.
[21] Lundborg G, Dahlin L. Anatomy, function, and pathophysiology of peripheral nerves and nerve compression. Hand Clin 1996;12:185–93.
[22] Kawamata S, Ozawa J, Hashimoto M, Kurose T, Shinohara H. Structure of the rat subcutaneous connective tissue in relation to its slide mechanism. Arch Histol Cytol 2003;66:273–9.
[23] Goldstein B, Sanders J. Skin response to repetitive mechanical stress: a new experimental model in pig. Arch Phys Med Rehabil 1998;79(3):265–72.
[24] Ando J, Kamiya A. Flow-dependent regulation of gene expression in vascular endothelial cells. Jpn Heart J 1996;37:19–32.
[25] Barakat A, Davies P. Mechanisms of shear stress transmission and transduction in endothelial cells. Chest 1998;114:58S–63S.
[26] Davies P, Dewey CF, Bussolari S, Gordon E, Gimbrone MA. Influence of hemodynamic forces on vascular endothelial function. in vitro studies of shear stress and pinocytosis in bovine aortic cells. J Clin Invest 1984;73:1121–9.
[27] Girard PR, Nerem RM. Endothelial cell signaling and cytoskeletal changes in response to shear stress. Front Med Biol Eng 1993;5:31–6.
[28] Zheng YP, Mak AF. An ultrasound indentation system for biomechanical properties assessment of soft tissues in-vivo. IEEE Trans Biomed Eng 1996;43(9):912–8.
[29] Rubin M, Bodner S, Binur N. An elastic-viscoplastic model for excised facial tissues. J Biomech Eng 1998;120(5):686–9.
[30] Serina E, Mote C, Rempel D. Force response of the fingertip pulp to repeated compression–effects of loading rate, loading angle and anthropometry. J Biomech 1997;30(10):1035–40.
[31] Jindrich DL, Zhou Y, Becker T, Dennerlein JT. Non-linear viscoelastic models predict fingertip pulp force-displacement characteristics during voluntary tapping. J Biomech 2003;36(4):497–503.
[32] Murai M, Lau HK, Pereira BP, Pho RW. A cadaver study on volume and surface area of the fingertip. J Hand Surg [Am] 1997;22(5):935–41.
[33] Bruhn H, Gyngell ML, Hanicke W, Merboldt KD, Frahm J. High-resolution fast low-angle shot magnetic resonance imaging of the normal hand. Skeletal Radiol 1991;20(4):259–65.
[34] Wu JZ, Dong RG, Welcome DE. Analysis of the point mechanical impedance of fingerpad in vibration. Med Eng Phys 2006;28(8):816–26.
[35] Fertis DG. Mechanical and structural vibration. New York, Chichester: John Wiley and Sons, Inc.; 1995.
[36] Wu JZ, Dong RG, Smutz WP. Effects of static compression on the vibration modes of a fingertip. J Low Freq Noise Vib Active Control 2002;21(4):229–43.
[37] Lemaitre J, Chaboche JL. Mechanics of solid materials. Cambridge/New York: Cambridge University Press; 1990.
[38] Bovenzi M, Franzinelli A, Strambi F. Prevalence of vibration-induced white finger and assessment of vibration exposure among travertine workers in italy. Int Arch Occup Environ Health 1988;61(1–2):25–34.
[39] Bovenzi M. Exposure-response relationship in the hand–arm vibration syndrome: an overview of current epidemiology research. Int Arch Occup Environ Health 1998;71(8):509–19.
[40] Bovenzi M, Lindsell CJ, Griffin MJ. Response of finger circulation to energy equivalent combinations of magnitude and duration of vibration. Occup Environ Med 2001;58(3):185–93.
[41] Dong RG, McDowell TW, Welcome DE, Wu JZ. Biodynamic response of human fingers in a power grip subjected to a random vibration. ASME J Biomech Eng 2004;126:446–56.
[42] Nolano M, Provitera V, Crisci C, Stancanelli A, Wendelschafer-Crabb G, Kennedy WR, Santoro L. Quantification of myelinated endings and mechanoreceptors in human digital skin. Ann Neurol 2003;54(2):197–205.
[43] Martin JH, Jessell TM. Modality coding in the somatic sensory system. In: Kandel E, Schwartz J, Jessell T, editors. Principles of neural science. 3rd ed.. Norwalk, Connecticut: Appleton and Lange; 1991. 344–7.
[44] Lundstrom R, Lindmark A. Effects of local vibration on tactile perception in the hands of dentists. J Low Freq Noise Vib 1982;1(1):1–11.
[45] Lundstrom R. Effects of local vibration transmitted from ultrasonic devices on vibrotactile perception in the hands of therapists. Ergonomics 1985;28:793–803.